CHARACTERIZATION OF ATOMIZED AND EXTRUDED Al$_{92}$Fe$_3$Cr$_2$Mn$_3$ ALLOY

C. Triveño Rios, J. B. Fogagnolo, C. Bolfarini, W. J. Botta and C. S. Kiminami

Materials Engineering Department, Federal University of São Carlos, S. P., Brazil

Abstract. Powders of the Al$_{92}$Fe$_3$Cr$_2$Mn$_3$ quaternary alloy were produced by spray atomization processing; then they were processed by warm extrusion to obtain extruded ingots. The results revealed that in both the powder particles and the extruded bulk samples, α-Al, quasicrystalline and intermetallic phases coexist. The quasicrystalline phase was observed as aggregates and its decomposition to crystalline phase occurs above 500 °C. Microstructural changes after extrusion were not observed, indicating that the quasicrystalline phase and the intermetallic compounds are stable against coarsening during the time and temperature of extrusion. The presence of micro-porosities after the extrusion is attributed to the spherical form of the powders and mainly to the high volume of intermetallic faceted-particles.

1. INTRODUCTION

Recent progresses in studies of bulk amorphous and nanostructured alloys have opened new opportunities to improve the strength of aluminium-rich alloys when processed by rapid solidification. It has been shown that amorphous Al alloys could present high tensile strength with good bending ductility [1,2]. Furthermore, various interesting nanostructures such as quasicrystalline nanoparticles dispersed in an aluminium matrix were associated with the high cooling rates (10^6 K/s) in the melt-spinning or atomization processes [3]. These nanocrystalline alloys exhibit higher tensile strengths of 500–800 MPa and higher ductility of 5–25% as compared with the conventional high strength Al-based alloys [4]. For melts-pun Al$_{92}$Mn$_6$Ce$_2$ alloy [5] values of strength as high as 1320 MPa have been reported. In the present study, we report the efforts for the development of bulk Al$_{92}$Fe$_3$Cr$_2$Mn$_3$ alloy containing quasicrystalline and intermetallic particles as constituent phases using atomization and hot-extrusion as processing route. This alloy has been chosen for investigation be-cause Fe, Cr and Mn all have low diffusivity and low equilibrium solubility in fcc-Al [6], that are the basic requirements for preventing Ostwald ripening [7] together with high melting points (1538 °C, 1907 °C, and 1246 °C, for Fe, Cr, and Mn, respectively) [6].

2. EXPERIMENTAL PROCEDURE

Pre-alloys of approximately 80 g with a nominal composition of Al$_{73.1}$Fe$_{10.1}$Cr$_{6.7}$Mn$_{10.1}$ (in at.%) were prepared from pure elements using arc melting under argon atmosphere. For spray atomization processing the pre-alloy was mixed with aluminium (99.8% of purity) to obtain the alloy with nominal composition of Al$_{92}$Fe$_3$Cr$_2$Mn$_3$. The mixture was melted in induction furnace using a graphite crucible. The alloy, superheated by ~250 °C (T_m = 860 °C) has been atomized by nitrogen, at pressure of 1.2 MPa, into a fine dispersion of micron-sized droplets. The rapidly solidified powder has been sieved and classified into different size ranges such as < 25 µm, 20-30 µm, 30-45 µm, 45-76 µm, 76-106 µm, 106-250 µm, and 250-450 µm. For extrusion

Corresponding author: Claudemiro Bolfarini, e-mail: cbolfa@power.ufscar.br

processing the amount of powders in the size ranges < 25 µm, 106-250 µm, and 250-450 µm, were insufficient. Pre-compacted powder cylinder billets, with diameter of 15 mm and height of ~25 mm, have been prepared for different particles size ranges and extruded at 350 °C, with an extrusion ratio of 5/1, and speed of extrusion of 14 mm/min. The microstructures of the atomized powders and longitudinal sections of warm extrusion ingots were analyzed by scanning electron microscopy (SEM), X-ray diffraction (XRD) using CuK_α radiation, and by differential scanning calorimetry (DSC).

3. RESULTS AND DISCUSSION

The size distribution of the Al$_{92}$Fe$_3$Cr$_2$Mn$_3$ powders produced by gas atomization followed a log-normal distribution. The cumulative size distribution of median mass particle diameter was $d_{50} = 76$ µm. Particles in the size range of few microns up to 180 µm, present spherical morphology, typical for gas atomized powder. However, other irregular morphologies were observed, such as a tendency to form flake and ellipsoid. Also small particles (satellites) attached to large particles has been observed (Fig. 1a). The presence of particles with different morphologies can be related to the Rayleigh instabilities [8] that depend on all the parameters involved in the process. The smaller particles (< 76 µm) showed preferentially a smooth surface whereas the larger particles tended to have a rough surface (Fig.1a).

The cross-sections of particles smaller than 30 µm in diameter, showed three types of microstructures (Fig. 1b). One type exhibiting grains of spherical shape (point B), the other exhibiting aggregates of grains (point C), and the last (point A) exhibiting the coexistence of intermetallic and α-Al phases. The first two types possibly correspond to quasicrystalline phases due to the nanometric size of the grains, smaller than 500 nm (point B). In the size range smaller than 76 mm in diameter, there was the same volume fraction of intermetallic and quasicrystalline phases, both embedded in a-Al matrix.

Fig. 1c shows star-like morphologies with 5 sides and 1.2 µm of diameter, structurally made of grains with sizes about 350 nm with each side corresponding to an arm irradiated from a centre. The morphology of these aggregates of grains corresponds to a polygon of five sides, suggesting that they assume the icosahedral form of quasicrystalline phases. That form of quasicrystalline grains preserving 5-fold symme-

try axis is also observed for size range of 20-45 µm (Fig. 1d), within grains of ~2.0 µm of diameter embedded in fcc-Al matrix. It is likely that they were also formed by grain aggregates, such as in Fig. 1c, but with morphologic changes from single star to flower-like or dendritic shapes, preserving the five sides or irradiated arms from a centre. It is reported [9] that icosahedral nucleus forms homogeneously in the liquid state and acts as a precursor for the formation and growth of crystalline phases. In the size range of 30-76 µm (Fig. 1e) it can be seen a growth of columnar dendrites with secondary arms arising from grain aggregates. It has been suggested that an anisotropic heat flux results in grain growth in preferred directions creating three-dimensional flower-like grains or dendrites [9,10]. These morphologic changes suggest decomposition from quasicrystalline to crystalline phase. However, the growth of these morphologic aggregates frequently reflects the shape of the noncrystallographic symmetry of the quasicrystals and possibly corresponds to 5-fold symmetry axis of icosahedral phase. On the other hand, in larger sizes (> 76 µm) the volume fraction of the intermetallic phases (Fig. 1f), it is predominant than the quasicrystalline phases. The morphology of the intermetallic phases is in the form hexagonal and faceted cuboids. The higher degree of undercooling experimented by particles constituted by apparent quasicrystalline phases due to higher cooling rates explain these differences in microstructures. EDS analysis of the phases showed that they have different compositions; ~Al$_{75.7}$Cr$_{8.2}$Mn$_{8.4}$Fe$_{7.7}$ and ~Al$_{82.8}$Mn$_{7.9}$Fe$_{7.9}$(Cr) (in at.%), which corresponds to quaternary (hexagonal platelets) and ternary metastable phases, respectively. These EDS/MEV analyses suggest that those phases present characteristics similar to the Al$_6$Mn and Al$_{12}$(Cr,Mn) phases identified from the JCPDS database. In this case, the Mn and Al are partially substituted by iron and chromium. However, the EDS/MEV analysis of flower-like grains was of ~Al$_{78}$Cr$_{5.8}$Mn$_{8.0}$Fe$_{8.2}$ and contains different solute contents than the Al$_{85}$Cr$_{2.1}$Mn$_{6.4}$Fe$_{4.3}$Ti$_{2.2}$ and Al$_{82.9}$Mn$_{6.3}$Fe$_{9.0}$Ti$_{1.8}$ icosahedral phases for the Al$_{93}$Mn$_3$Fe$_2$Cr$_1$Ti$_1$ and Al$_{93}$Mn$_2$Fe$_3$Ti$_2$ alloys [11], respectively. These results suggest that the icosahedral phase is not a stoichiometric compound and that it exists over a significant range of compositions.

The consolidation process showed the three stages characteristics of powder extrusion, as described elsewhere [12]. By decreasing the particles size ranges from 76-106 µm to 20-30 µm an in-
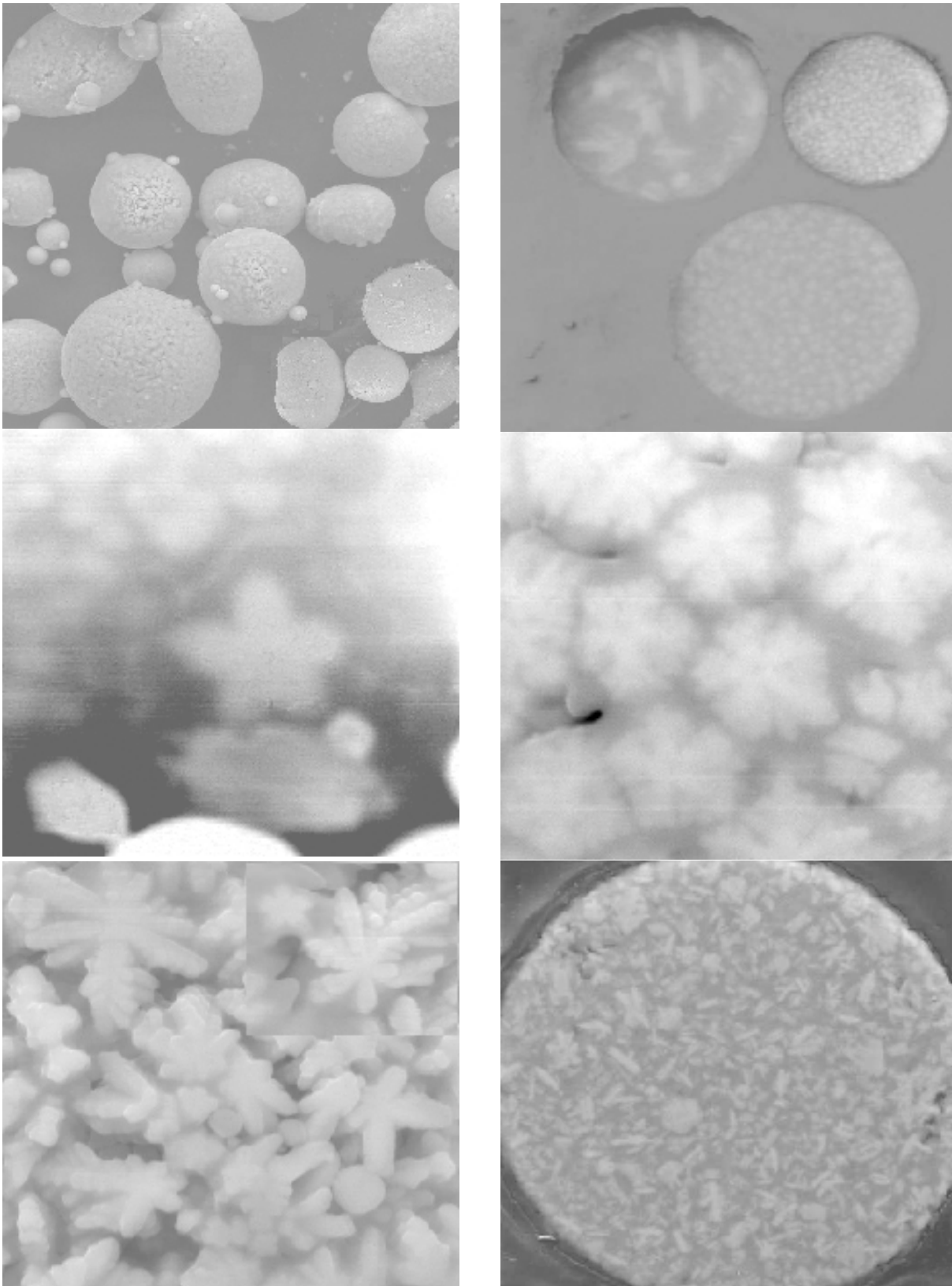
Fig. 1. SEM micrograph of as-atomized $Al_{92}Fe_3Cr_2Mn_3$ powders showing; (a) typical morphology and different surfaces of powder particles; (b) transversal section of particles (< 30 μm), showing presence of intermetallic phases (A), spherical grains of apparent quasicrystalline phase (B), and grain aggregates (C); (c) star-like morphology observed in particles < 30 μm; (d) flower-like morphology with 5-arms observed in particles of 20-45 μm; (e) columnar dendrites observed in particles of 30-76 μm, and (f) transversal section of particles (> 106 μm), showing presence of intermetallic phases.
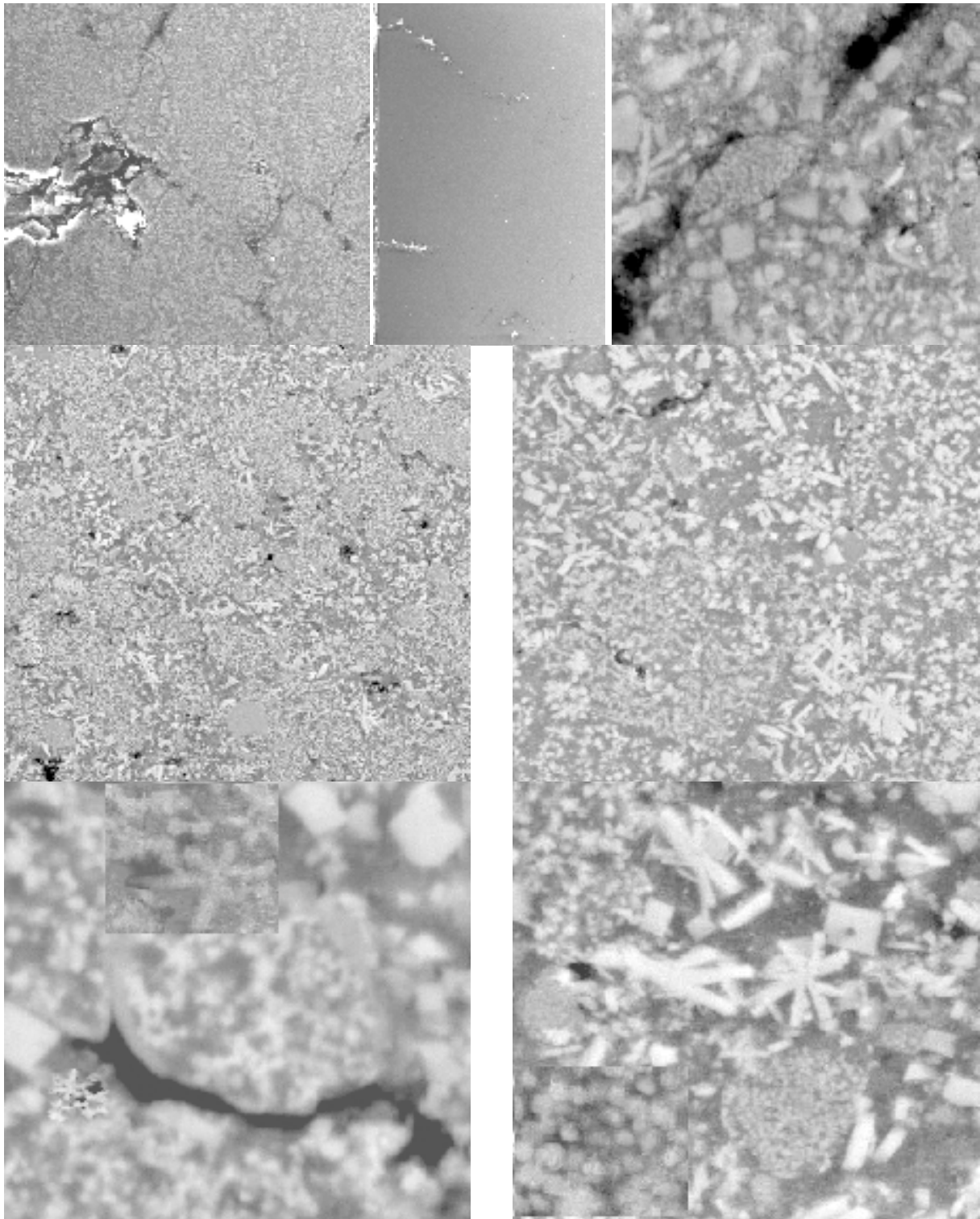
Fig. 2. SEM images of the longitudinal section of the product extruded. (a-c) Crack propagation in close regions to the beginning and end of the crack, (b) Periphery region with lateral cracks and extrusion direction. Transversal sections of size fractions of; (d) 20-30 μm, (e) 75-106 μm, e (f-g) magnification of Fig. 2d. Inset in figures d-e show grains in star shape and quasicrystalline grains.

crease of the maximum load has been observed, from 655 MPa to 753 MPa respectively. The extru-sion pressure increases with decreasing powder particle size.
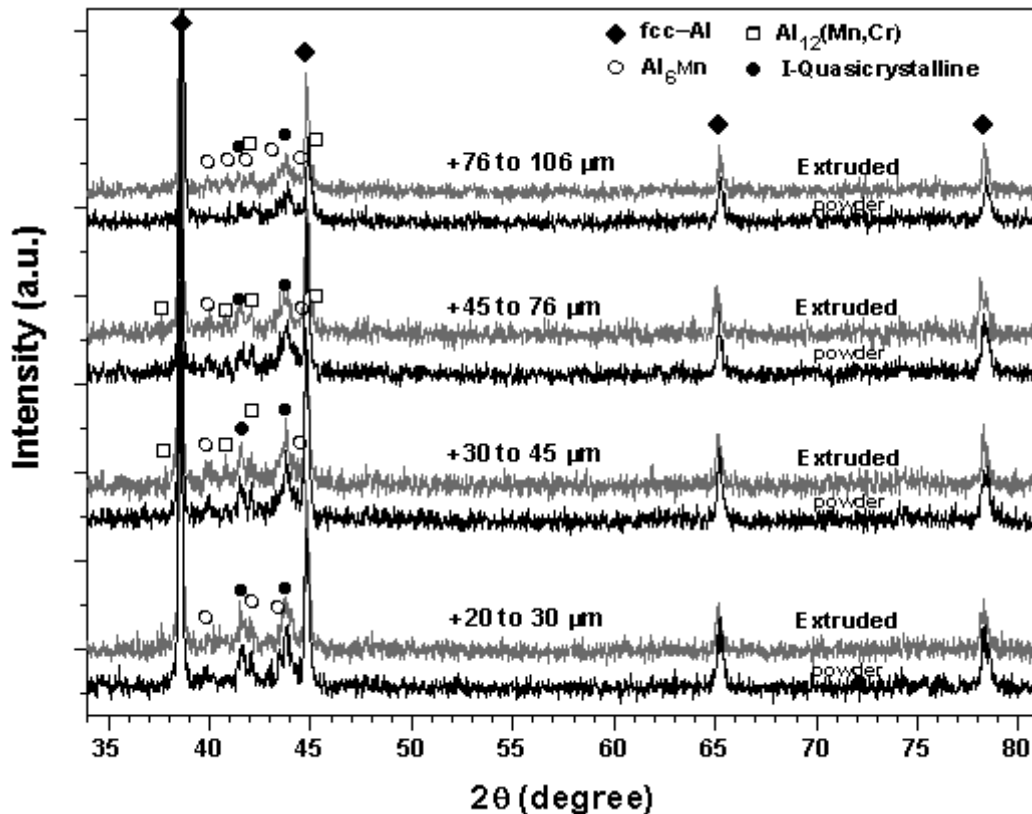
Fig. 3. XRD patterns taken from powders and their respective extrudated produced at 350 °C and ratio of 5:1, in the size fractions of 20-30, 30-45, 45- 76, and 76-106 μm.

Figs. 2a-2c show pictures of the longitudinal section of the product extruded. One can see small lateral cracks with lengths within of 900 μm and spaced at nearly 1.0 mm, which are more open in the periphery of extruded ingots. This defect may be linked with the reduction rate (5:1), extrusion temperature (350 °C) and lubrication conditions, that do not satisfy of way optimized the extrusion process. The cracks propagate in preferential way through the powder/powder interface (Fig. 2a). Fig. 2c illustrates a particle of quasicrystalline grains which acts as an obstacle to the propagation of cracks. This is evidence that the bonding energy is smaller at the interface of the powder particles than through of the intra-particles. Also, it was observed that the spherical or near-spherical shape of the powder particles without any preferred alignment at the die entry have undergone severe shape changes into particles elongated, along the extruded ingots, which tend to align with the extrusion direction towards the die exit, such as showed in the figures 2a. This observation is in agreement with the work of Bouchaud *et al.* [13] who explain it by the matrix flow forcing the particles to align with the extrusion direction. Figs. 2e and 2f correspond to the cross section of the extruded sample using 20-30 and 75-106 μm size range particles, respectively. It is observed a cellular structure with the presence of intermetallic phases around the cell boundaries. It is clear from this picture that the bonding between the powder particles has taken place leading to densification. However, in addition to bonding, the microstructure revealed presence of microporosities around the particles boundaries (or cellular interfaces). The volume fraction of the microporosities was larger in the 20-30 μm range with ~2.1±0.6% (Fig. 2d), decreasing for ~1.0±0.5% in the 75-106 μm range (Fig. 2e). The presence of microporosities can be associated with incomplete densification, as well as, to the perfect sphericity of the powders at the smaller size range, and to the high volume fraction of the various faceted intermetallic compounds of high hardness and low deformability in the particles-boundaries. Such
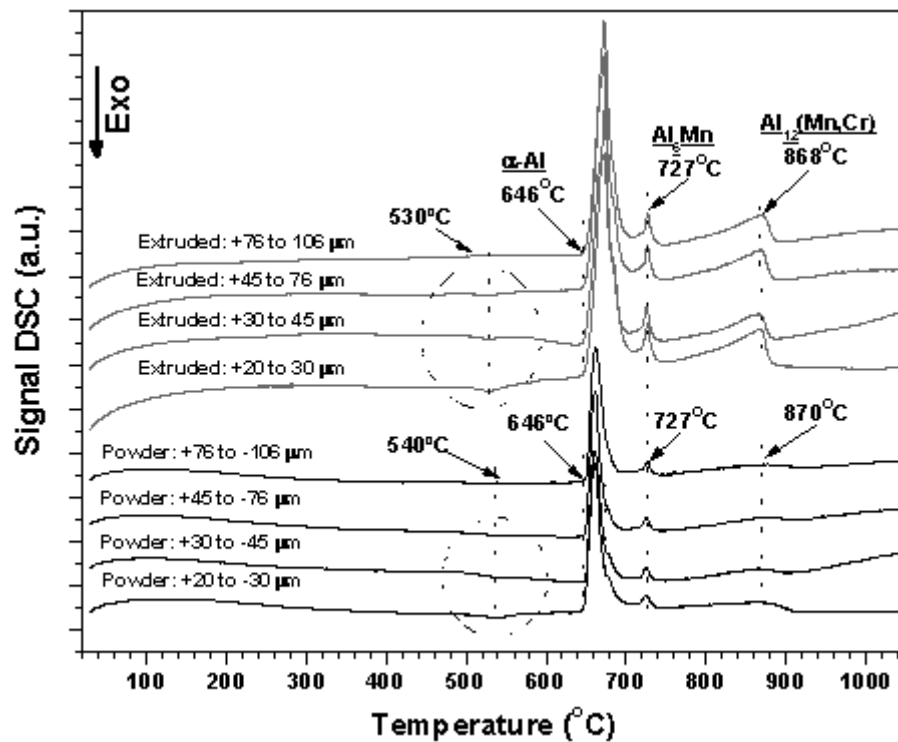
Fig. 4. DSC curves taken from powders and their respective extrudated produced at 350 °C and ratio of 5:1, in the size fractions of 20-30, 30-45, 45- 76, and 76-106 μm, heated at 20 K/min.

compounds are obstacles for the deformation of the particles, preventing the connection and bonding among the powder particles, such as observed in Figs. 2f and 2g.

The size and form of the phases observed in the ingots after the extrusion process were similar to the ones presented in the atomized powder particles (Figs. 2d-2g). It indicates that the microstructure was maintained after extrusion. In this case, the apparent quasicrystalline phase with "star" shape (inset in Fig. 2f) and quasicrystalline grains of spherical shape with sizes smaller than 500 nm maintain their size and shape (inset in Fig. 2g) at all size fractions after extrusion. The same behaviour is observed with the intermetallic compounds. This microstructural stability is in agreement with the XRD patterns presented in Fig. 3, which shows only a slight shift of the α-Al peaks to lower values of 2θ of α-Al (indicative of higher lattice parameter), and a slight decrease in the peak broadening (indicative of a reduction in solid solution levels of Mn, Cr, and Fe elements), wich are resulting from the extrusion time at the processing temperature. In fact, this behaviour is also in agree-

ment with the DSC thermograms (Fig. 4) for the powder and extruded-ingots, where it is showed exothermic peaks at 530 and 540 °C, respectively, indicating the phase transition from quasicrystalline to crystalline phase. This indicates that the extrusion temperature (350 °C) was much lower than the temperature of decomposition of the quasicrystalline phase. On the other hand, the microstructural stability is also related to the low interfacial energy of quasicrystals [14], and to the low self diffusion rate below a critical ordering temperature of the intermetallic compounds [15], which reduces the driving force for the growth, leading to the stable size of the particles. These factors may be responsible for the negligible coarsening of the quasicrystalline phase and of the intermetallic compounds during extrusion.

4. CONCLUSIONS

Powders of a previously prepared Al$_{92}$Fe$_3$Cr$_2$Mn$_3$ alloy were been produced via gas atomization and then consolidated by hot-extrusion. The microstructure of the smaller size powders (< 76 μm) is con-

stituted by; α-Al matrix as predominant phase, and in smaller proportion by grains with different morphologies that correspond to apparent quasicrystalline phases and by metastable intermetallic phases. However, in the larger size particles the intermetallic phases were more predominant that the grains of apparent quasicrystalline phase. Those differences can be attributed to the way of solidification of the particles. After the extrusion process it is concluded that the shape and size of grains and intermetallic phases, it is similar to the observed in the as-atomized powders, indicating good microstructural stability up to 350 °C. The formation of microporosities and surface defects (cracks) can be related to the reduction rate, extrusion temperature and lubrication conditions, that don't lead to the optimization of the extrusion process. The formation of microporosities, also can be attributed to the powder spherical form and mainly to the high volume of intermetallic fateted-particles. Therefore, a combination of high volume fraction of intermetallic phases with smaller fraction of apparent quasicrystalline phases at extruded products, should affect considerably its mechanical properties.

ACKNOWLEDGEMENTS

REFERENCES

[1] A. Inoue, K. Ohtera and T. Masumoto // *Jpn. J. Appl. Phys.* **27** (1988) L736.
[2] A. Inoue, K. Ohtera, A. P. Tsai and T. Masumoto // *Jpn J. Appl. Phys.* **27** (1988) L280.
[3] J. Q. Guo and K. Ohtera // *Acta Mater.* **46** (1998) 3829.
[4] A. Inoue and H. M. Kimura // *Mat. Sci. Eng. A* **286** (2000) 1.
[5] A. Inoue, M. Watanabe, H.M. Kimura, F. Takahashi, A. Nagata and T. Masumoto // *Mater. Trans. JIM* **33** (1992) 723.
[6] T. B. Massalski, *Binary alloy phase diagrams, 2nd ed.* (Materials Park,OH: ASM International, Materials Park, 1990).
[7] C. Wagner // *Elektrochem. Z.* **65** (1961) 581.
[8] R. M. German, *Powder Metallurgy Science, 2nd ed.* (New Jersey, 1994).
[9] A. K. Srivastava and S. Ranganathan // *Acta Mater.* **44** (1996) 2935.
[10] W. J. Boettinger, D. Shechtman, R. J. Shaeffer and F. S. Biancaniello // *Metall. Trans.* **15A** (1984) 1129.
[11] H. M. Kimura, K. Sasamori and A. Inoue // *J. Mater. Res* **15** (2000) 2737.
[12] P. R. Roberts and B. L. Ferguson // *Int. Mater. Rev.* **36** (1991) 62.
[13] E. Bouchaud, L. Kubin and H. Octor // *Metall. Trans. A.* **22A** (1991) 1021.
[14] C. Janot, *Quasicrystals* (Clarendon Press, Oxford, 1994).
[15] K. S. Kumar // *Inter. Mater. Rev.* **35** (1990) 293.